International Journal of Mining Science and Technology 26 (2016) 471–476

Contents lists available at ScienceDirect

International Journal of Mining Science and Technology

journal homepage: www.elsevier.com/locate/ijmst

Analysis of roof and pillar failure associated with weak floor at a limestone mine

Murphy Michael M. [a,*], Ellenberger John L. [a], Esterhuizen Gabriel S. [a], Miller Tim [b]

[a] Office of Mine Safety and Health Research, National Institute of Occupational Safety and Health, Pittsburgh, PA 15228, USA
[b] East Fairfield Company, North Lima, OH, USA

ARTICLE INFO

Article history:
Received 7 June 2015
Received in revised form 16 August 2015
Accepted 3 November 2015
Available online 15 March 2016

Keywords:
Underground limestone
Ground control
Case study
Weak floor
Instability

ABSTRACT

A limestone mine in Ohio has had instability problems that have led to massive roof falls extending to the surface. This study focuses on the role that weak, moisture-sensitive floor has in the instability issues. Previous NIOSH research related to this subject did not include analysis for weak floor or weak bands and recommended that when such issues arise they should be investigated further using a more advanced analysis. Therefore, to further investigate the observed instability occurring on a large scale at the Ohio mine, FLAC3D numerical models were employed to demonstrate the effect that a weak floor has on roof and pillar stability. This case study will provide important information to limestone mine operators regarding the impact of weak floor causing the potential for roof collapse, pillar failure, and subsequent subsidence of the ground surface.

1. Introduction

Massive roof falls extending to the surface at a limestone mine in Ohio have been studied collaboratively by the National Institute for Occupational Safety and Health (NIOSH) and the mine owners. This paper provides a summary of the sequence of events leading to observed instability and presents a numerical modeling analysis that investigates the role a weak floor can have on roof and pillar stability.

This study builds upon previous NIOSH research in underground limestone mines undertaken by way of a survey that analyzed performance of pillars in 34 different stone mines in the Eastern and Midwestern United States between 2005 and 2009 [1]. This survey led to the development of underground stone mine pillar design guidelines based upon a "stability factor" for the pillar system. The factor is compared to operational experience to determine ranges of values that are typical of stable pillar systems. A software package titled Stone mine pillar design (S-pillar) was developed for easy application of these guidelines [2].

Weak floor in the present case study departs significantly from cases included in the previous NIOSH research, in that none of the 34 study mines had weak floor issues. Moreover, this case study is the first in which a weak floor has been monitored routinely as roof falls are occurring. A detailed report on the observations and measurements taken at the mine has been published [3]. The previous observations led to the conclusion that although there were weak bands in the pillar, the weak floor was the significant defect that led to the instability issues. The pillars were initially mined in 2004, approximately 10 years before the instability issues began to occur. The objective of this study is to use numerical models to analyze a variety of floor strengths and the impact of moisture content to find the critical point at which the floor becomes unstable, leading to long-term instability issues.

2. Site description and field observations

The study site is the Petersburg Mine, an underground limestone mine owned by East Fairfield Coal Company, located in eastern Ohio in Mahoning County. The mining horizon is generally from 60 to 75 m below the surface. The mine is developed from a box cut, with portals into the Vanport limestone seam with slightly less than 45 m of overburden. The surface is gently rolling, and the Vanport limestone remains near horizontal with maximum grades of less than three degrees. Geologically, the Vanport limestone is a part of the Allegheny Formation within the Pennsylvanian System. The lower Kittanning coal overlies the Vanport limestone and is typically 9–12 m above the top of the limestone.

The underground mine design incorporated a variety of pillar sizes, but generally consisted of 12 m wide drifts driven directly west with north–south crosscuts that were also 12 m wide. The pillars were 8 m wide by 18 m long. The resultant mine plan

* Corresponding author. Tel.: +1 412 3864172.
E-mail addresses: MMMurphy@cdc.gov, mmu5@cdc.gov (M.M. Murphy).

http://dx.doi.org/10.1016/j.ijmst.2016.02.016
2095-2686/

consisted of crosscuts on 30 m centers with drifts on 19.8 m centers. The initial mining height was approximately 5.5 m, leaving a 1.2 m beam of limestone in the immediate roof.

Typically, the mine leaves approximately 0.6 m of limestone in the floor. However, in the area of the instability, it was observed that less than 0.6 m of limestone had been left in the floor. The mine geologist indicated that the stone thickness at the bottom of the pillar changed irregularly due to dips, resulting in a thinner floor stone thickness than what was planned. Borehole logs in this area showed that a 1 m thick weak unit of moisture-sensitive fireclay was beneath the limestone but not present in other parts of the mine. The fireclay was a rock when it was cored, however, upon weathering it turned into a soft and crumbly material, as described by the mine geologist. This fireclay floor bed could not be tested for a uniaxial compressive strength test, because the core pieces were too small for analysis. However, the strength was estimated to be 3 MPa by NIOSH based on field evaluation methods [4]. Also during the field evaluation, the weak floor unit appeared to have a consistency of a stiff soil and contained clayey minerals. In a few areas, the pillars were standing directly on top of this weak bed. The site geologist also mentioned that this area had standing water multiple times in the past.

A team of NIOSH researchers made routine visits to the mine to collect data and gain insight into the causes behind the instability. Through previous observational and numerical analysis detailed in Murphy et al., the major factors that led to the instability are as follows [3]:

(1) Less than 0.6 m of limestone was left in the floor in some areas, leading to the exposure of a weak, moisture-sensitive fireclay unit below;
(2) Yielding of the weak floor induced tensile fracturing in the bottom section of the pillar;
(3) Due to the tensile fracturing, the pillar began to slough off at the corners and major blocks fell off from around the pillar;
(4) A weak band located near the mid-height of the pillar was able to squeeze out, inducing more tensile fracturing in the upper portion of the pillar. In some cases, the upper portion also experienced sloughing or scaling;
(5) Due to the decreased size of the pillar through sloughing, the effective footprint of the pillar and its load-bearing capacity were reduced. Thus the pillar was able to punch further into the floor, resulting in floor heave;
(6) After a number of adjacent pillars began to punch into the floor, a wide area roof collapse occurred. Due to the weak shale above the limestone roof beam, the fall extended to the surface.

3. Stability analysis

The NIOSH developed S-pillar software was initially used to estimate the stability of a typical pillar found in the Vanport limestone seam using the mining dimensions at the Petersburg Mine. The S-pillar analysis does not take into account the defects within the pillar or the weak floor, but will give a stability factor for a solid pillar on top of a competent floor. S-pillar was also used to find the estimated stress in the pillars, due to the depth and excavation, which could be expected at the Petersburg Mine.

After the stability was determined for the solid pillar, the S-pillar software was the starting point to calibrate a series of FLAC3D Mohr–Coulomb strain softening numerical models. To begin, a FLAC3D numerical model was created to represent a limestone pillar with a similar Uniaxial Compressive Strength (UCS) measured from the Vanport limestone seam. The objective was to match the strength of the solid pillar calculated in S-pillar to the strength of a solid pillar simulated in the FLAC3D numerical model. In this study, a solid pillar is defined as a Vanport limestone seam pillar with intact rock and does not include any defects such as a weak band.

Once the solid Vanport limestone seam pillar was calibrated in FLAC3D, the weak band defects were added into the model. The pillars that included the weak bands were representative of the typical pillar structure found in the areas of instability at the Petersburg Mine. For this study, the pillars that included weak bands observed in the areas of instability were defined as the Vanport limestone seam pillars with defects.

Initially during this analysis, the floor remained competent and strong. The objective was to analyze the reduced stability due to the weak bands prior to analyzing the impact of a weak floor. Next, a series of models were analyzed where floor directly below the pillars with defects had its strength slowly reduced. The objective was to find a critical floor strength that caused instability to the full system (roof, pillar, and floor). Finally, a series of models were analyzed where increasing moisture content and pore-pressure effects were simulated by decreasing the effective friction angle inthe floor. The objective was to analyze the impact of moisture in the floor to the instability in the full system.

3.1. S-pillar strength calculation for the solid Vanport limestone seam pillar

The S-pillar software uses an empirically based method to calculate a stability factor for stone mine designs. Included in the S-pillar analysis is an equation used to calculate the pillar strength that takes into consideration the laboratory uniaxial compressive strength, large discontinuities, pillar width, and pillar height. S-pillar was used as a starting point for this study to estimate the strength of a solid Vanport limestone seam pillar and the tributary area stress caused by the excavation dimensions and depth used at the Petersburg Mine.

After adding the mining dimensions of the Petersburg Mine and geotechnical properties of the Vanport limestone seam into S-pillar, the software estimated the pillar strength to be 39.4 MPa, as shown in Fig. 1.

The factor of safety using these mining dimensions and seam properties was calculated to be 5.87. Therefore, the tributary area stress approximation could be back-calculated using the pillar strength. The approximate stress in the pillar was calculated to be 6.71 MPa. For the scenarios analyzed in this study, the critical floor strength was determined at the value that caused the pillar strength to fall below 6.71 MPa.

3.2. FLAC3D calibration of the solid Vanport limestone seam pillar

A FLAC3D Mohr–Coulomb strain softening numerical model was created to estimate the strength of a solid Vanport limestone

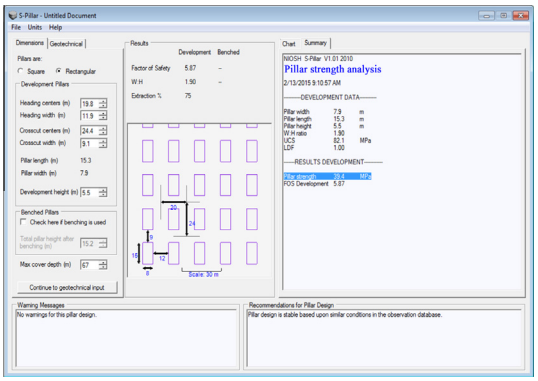

Fig. 1. S-Pillar strength analysis results for a solid Vanport limestone seam pillar.

seam pillar, consisting of intact rock with a uniaxial compressive strength of 82 MPa, a value based on NIOSH laboratory testing. The Coulomb strength parameters of the full-scale rock mass were estimated using a geological strength index of 80 units, after Esterhuizen and Ellenberger [5,6]. The roof and floor were created with the same modulus properties as the pillar; however, they were set to be elastic so that the failure was contained within the pillar. The full set of mechanical properties used for this model is shown in Table 1.

To find the strength of the pillar in the model, the following approach was taken:

- The model was not made to represent a full 3D pillar, but rather a 2D slice with a thickness of 1.2 m through a section of the pillar.
- The element size in the pillar and the rock units directly above and below the pillar were approximately 15 cm. The element sizes near the upper and lower boundaries of the model were increased to 30 cm.
- The upper and lower boundaries of the model were constrained in the vertical direction and a symmetry plane was defined at the left and right boundaries.
- Interfaces with a low cohesion and friction angle were used between each rock unit. For all of the models analyzed in this study, the interface friction angle was set to 20° and the interface cohesion was set to 0.1 MPa.
- The major horizontal stress was set to twice the vertical stress, with the minor horizontal stress set equal to the vertical stress, which is typical for this region.
- Once the stresses were initialized, the entries were mined-out to form the pillar. The excavation of the entries was simulated by gradually reducing the pre-mining pressure along the boundaries of the excavation. The model was then allowed to come to equilibrium under gravity loading.
- Once in equilibrium, the upper boundary constraint was removed and a constant velocity was applied at the top to slowly load to the pillar in a quasi-static manner.
- As the pillar was loaded, the cohesion and tension properties were reduced to 10% of their full strength at 5 m ill strain. At 10 m ill strain, both properties were set to a residual strength of 1 kPa.
- The pillar was loaded to failure and a resulting stress–strain curve was created. The stress was measured by monitoring and averaging five locations across the pillar at approximately mid-height. The change in length of the pillar, needed for the strain calculation, was found by monitoring the displacement at the top and bottom of the pillar.

The stress–strain curve from the FLAC3D solid Vanport limestone seam pillar is shown in Fig. 2. According to the stress–strain curve, the field strength of the pillar was found to be 39.03 MPa. The strength found using the numerical modeling approach is in agreement with the empirically based S-pillar calculation, which calculated the strength at 39.4 MPa. This result verifies that the modeling approach used in FLAC3D accurately represents a typical solid Vanport limestone seam pillar and can be used to further evaluate the effects of weak bands and weak floor.

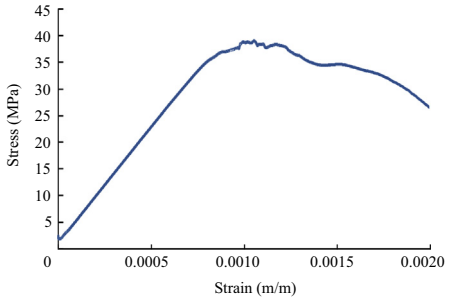

Fig. 2. Stress–strain curve for a FLAC3D solid Vanport limestone seam pillar.

3.3. FLAC3D analysis of the Vanport limestone seam pillars with defects on top of a competent floor

Observations made at the mine indicated that the pillars were not solid because of weak bands within the pillar and a blockier bottom section of the pillar [3]. A FLAC3D Mohr–Coulomb strain softening numerical model was created to evaluate the effect of these two defects within the pillar. The pillar consists of four units. The top two units consist of limestone with a moderate uniaxial compressive strength of 82 MPa. Again, this was the value measured from laboratory testing of the Vanport limestone seam. In the field, there was a very thin weak band observed in the upper portion of the pillar. In the model, this was represented by an interface with low cohesion and friction angle between the top two units of the 82 MPa limestone. A weak band just under the mid-height of the pillar was modeled as a strong, clayey soil, and properties were obtained from a previous study that showed the effect of weak bands in a limestone pillar [6]. The bottom portion of the pillar was a blocky limestone and was modeled assuming it had a reduced geologic strength index of 40, giving overall lower values for the Mohr–Coulomb parameters when compared to the stronger units at the top of the pillar.

The model also incorporates the roof geology that was observed at the mine. The immediate roof above the pillar consists of a 1.2 m beam of 82 MPa limestone. Above the limestone beam was shale extending to the surface, with an estimated UCS of 40 MPa based on field evaluation methods. The associated 40 MPa shale Coulomb strength parameters were found using NIOSH-developed and calibrated procedures described in Zipf and Esterhuizen [7,8]. The floor remained competent for this part of the analysis and was given the 82 MPa limestone properties. The objective for this model was to analyze the reduction in stability only from the defects found within the pillar. The full set of properties used for this analysis is shown in Table 2. The modeled roof, floor, and pillar are shown in Fig. 3, along with a conceptual drawing of the pillar units and corresponding photograph.

The model was initialized and loaded to failure in the same manner described in the previous section. A stress–strain curve was developed and is shown in Fig. 4. In Fig. 4, the strength of pillars with defects is compared to the previously modeled solid Vanport seam pillar. The critical stress line is the limit at which the pillar will fail from the stress caused by the depth and excavation, as calculated from S-pillar.

Table 1
Descriptions and mechanical properties of the rock units used in the FLAC3D numerical model to calibrate the strength of the solid Vanport limestone seam pillar.

Unit description	Thickness (m)	Young's modulus (GPa)	Poisson's ratio	Cohesion (MPa)	Tension (MPa)	Friction angle (°)	Dilation angle (°)
82 MPa limestone roof (elastic)	21.2	40	0.25				
82 MPa limestone solid pillar	5.50	40	0.25	8.83	1.00	38	5
82 MPa limestone floor (elastic)	16.0	40	0.25				

Table 2
Descriptions and mechanical properties of the rock units used in the FLAC3D numerical model to analyze the pillars with defects on top of a competent floor.

Unit description		Thickness (m)	Young's modulus (GPa)	Poisson's ratio	Cohesion (MPa)	Tension (MPa)	Friction angle (°)	Dilation angle (°)
Roof	40 MPa shale	20	12	0.25	5.230	1.74	28	5
	82 MPa limestone	1.2	40	0.25	8.830	1.00	38	5
Pillar	82 MPa limestone	1.6	40	0.25	8.830	1.00	38	5
	82 MPa limestone	1.8	40	0.25	8.830	1.00	38	5
	Weak band	0.3	2	0.25	0.006	0.31	24	5
	82 MPa blocky limestone	1.8	35	0.25	1.000	0.33	34	5
Floor	82 MPa limestone	1.2	40	0.25	8.830	1.00	38	5
	82 MPa limestone	15.0	40	0.25	8.830	1.00	38	5

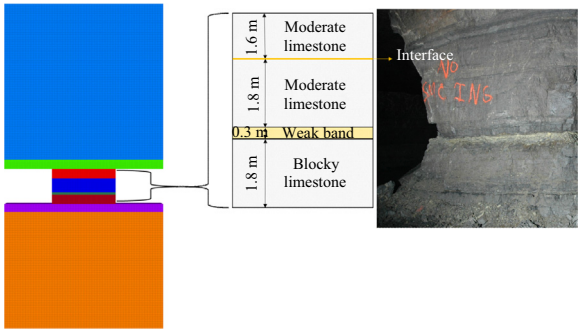

Fig. 3. Description of pillar units evaluated in the Mohr–Coulomb strain softening FLAC3D model.

The pillars with defects curve shows a significant strength reduction when the weak bands and blocky bottom portion of the pillar are taken into account. Although weak bands are known to reduce the load-bearing capacity in pillars, these model results show that the pillars with defects are able to remain stable despite having the weak bands and blocky bottom unit [7]. This agrees with observations at the mine, since there are stable pillars with these defects standing on acompetent limestone floor.

3.4. FLAC3D analysis of reducing the floor strength

Observations at the mine led to the conclusion that the main driver for the instability was the weak floor [3]. A series of FLAC3D numerical models were developed where the strength of the floor was reduced to find the critical point at which the pillar became unstable. The roof and pillar were modeled in the same way as described in Fig. 3; however, the first 1 m of the floor was weakened over the series of models. Below the first 1 m of the floor, the material remained constant.At the mine, some pillars were standing on limestone with a thickness of less than 0.6 m, while other pillars were standing directly on the weak floor material. The numerical modeling analysis only considered the scenarios where the pillars were directly standing on the weak floor material so that less complexity is included in the model.

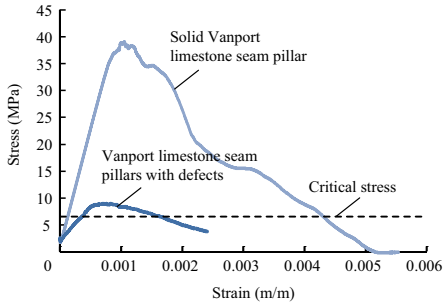

Fig. 4. Stress–strain curve comparison for the solid Vanport limestone seam pillar vs. Vanport limestone seam pillars with defects.

The properties for this series of numerical models are the same as found in Table 2, except for the material used in the first 1 m of the floor. The different strengths used for the first 1 m of the floor can be seen in Table 3, with their associated mechanical properties. The properties were based on the uniaxial compressive strength and created using calibrated methods found in Zipf and Esterhuizen [7,8]. The lowest strength modeled was 3 MPa, which was the assumed strength of the floor based on field evaluation methods at the mine.

The effect of the floor strength on the pillars was observed by loading the pillars until they failed in the same way as in the previous models. A stress–strain curve of the pillar was developed for each floor strength and is shown in Fig. 5. In Fig. 5, the stress–strain curve for the pillar with defects on the competent limestone floor (from Fig. 4) is shown for comparison. The critical stress line is the limit at which the pillar will fail fromthe stress caused by the depth and excavation, as calculated from S-pillar.

The stress–strain curves indicate that weakening the strength of the floor has an effect on the strength of the pillar. As the floor strength is reduced, the peak strength of the pillars comes closer to the critical stress. The weakest floor modeled has a Uniaxial Compressive Strength (UCS) of 3 MPa, similar to the floor strength estimated by field methods in the mine. This floor material causes the pillar strength to be similar to the critical stress, indicating that this floor strength is at the critical point to cause instability at the mine. This analysis suggests that the floor strength must be significantly reduced in order to cause the pillars to fail under the critical stress. At the mine, some pillars were in direct contact with the weak floor bed, but the pillars remained stable for 10 years prior to instability issues. It is possible that the floor weakened over time (mainly due to wet/dry cycles that occurred in the areas of instability) until it was reduced to the critical floor strength that resulted in instability.

3.5. FLAC3D analysis of the effect of moisture in the floor

The previous models indicated that the observed 3 MPa floor material could reduce the pillar strength to a critical point. However, these models represented a weak floor that was considered to be dry. It is believed that at the mine, the floor strength may have been further reduced due to an increase in moisture content. To account for this, a series of numerical models were developed where the effect of moisture content in the floor was simulated. The model was setup in the same way as in Fig. 3; however, the first 1 m of the floor was modeled using the 3 MPa floor properties (Table 3) while simulating the effect of moisture content. To simulate increasing moisture content and pore-pressure effects, the

Table 3
Mechanical properties of the different floor strengths used in the FLAC3D numerical models.

Floor strength	Poisson's ratio	Young's modulus (GPa)	Cohesion (MPa)	Tension (MPa)	Friction angle (°)	Dilation angle (°)
30 MPa	0.25	12	5.2270	1.7420	28	5
20 MPa	0.25	10	3.6950	1.2320	25	5
15 MPa	0.25	6	2.7710	0.9238	25	5
10 MPa	0.25	6	1.8480	0.6158	25	5
5.0 MPa	0.25	5	0.9238	0.3079	25	5
3.0 MPa	0.25	5	0.5543	0.1848	25	5

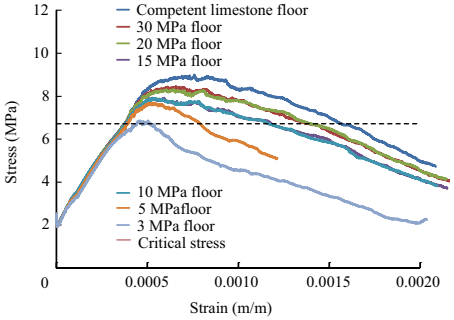

Fig. 5. Stress–strain curve comparison of reducing the floor strength in the first 1 m directly underneath the Vanport limestone seam pillars with defects.

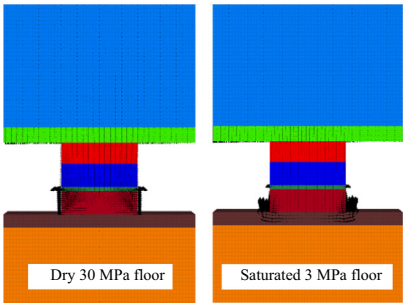

Fig. 7. Velocity vectors showing the failure movement of the pillar for a dry 30 MPa floor and a saturated 3 MPa floor.

effective friction angle of the 3 MPa floor was reduced. The friction angles used for these series of models were 25°, 20°, 15°, 10°, and 5°. The model using the 25° friction angle is considered to be a "dry" floor since it uses the original calibrated properties for the UCS. The effect of moisture in the floor was determined by loading the pillars until they failed in the same way as in the previous models. The peak strength of the pillars was measured for each floor with a varying friction angle and is shown in Fig. 6. The critical stress is indicated on the plot by the dashed red line.

The model results demonstrate that as the moisture content is increased in the 3 MPa floor (simulated by reducing the friction angle), the pillar strength is significantly reduced to well below the critical stress. These results support the assumption that the wet/dry cycles in the mine were able to contribute to the weakening of the floor that led to the instability.

3.6. Discussion of stability analysis

The numerical models developed for this study confirmed that a weak, moisture-sensitive floor had a significant effect on the mine stability. At the mine, the openings had been stable for approximately 10 years before the instability issues started to occur. The models showed that a pillar with weak bands on top of a low-strength floor can remain stable (Fig. 5). However, when the floor strength was reduced significantly and the effect of moisture content was added into the models then the pillar strength fell below the critical stress (Fig. 6). At the study site, it is believed that the exposed low-strength floor became even weaker over time due to periods of standing water that was contained in the mine entries. For this mine, the models verify that a 3 MPa floor was the critical floor strength that led to significant instability. This strength is similar to the estimated strength of the stiff soil-like material observed below the pillars in the mine.

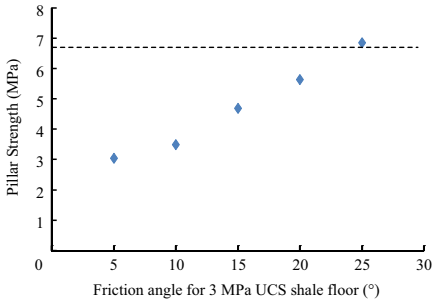

Fig. 6. Plot showing the reduction in pillar strength as the increasing moisture content reduces the effective friction angle of the floor material.

During the field site visits, it was observed that the pillar was able to punch into the floor, resulting in floor heave. It was also observed that on two separate occasions, two major roof falls were preceded by significant floor heave approximately a week before the instability [3]. A plot was created from the models to visually demonstrate the effect of a weak floor. In Fig. 7, velocity vectors are plotted for two scenarios: one where a dry, 30 MPa floor material was modeled and one where a saturated (friction angle reduced to 5°) 3 MPa floor material was modeled. The plots were created after the pillars had been loaded to failure. The velocity vectors give indication to where the failure was occurring based upon the grid point movement. On the left figure of Fig. 7, the black velocity vectors indicate that the weak band had squeezed out of the pillar and that the bottom, blocky portion of the pillar was heavily damaged through crushing. On the right figure of Fig. 7, significant floor heave can be seen, as indicated by the arrow vectors on the left and right sides of the pillar. The bottom portion of this pillar experienced more tensile failure due to punching into the saturated floor, causing the floor to heave around the sides of the pillar. These model results agree with observations seen at the mine where floor heave was used as an indicator that instability was approaching.

4. Conclusions

A limestone mine in Ohio has had roof instability problems that have led to massive roof falls extending to the surface. At the mine, the pillars in the area of instability were stable for 10 years prior to the major roof falls occurring. A team of NIOSH researchers has made routine visits to the mine to collect data and gain insight into the causes behind the instability. The resulting analysis indicated

that the pillars were able to remain in a critical state of stability when the weak floor was present. It was estimated through field methods that the weak floor with the consistency of a stiff soil had a uniaxial compressive strength of about 3 MPa, which put the pillars in a critical state. Adding moisture or repeated wetting and drying may have caused further weakening of the floor, leading to the initiation of the pillars punching into the floor after 10 years. These findings show that when a weak floor is exposed in a limestone mine, the long-term stability of the underground openings could become questionable if the floor is sensitive to moisture. It is recommended that if a weak floor bed is encountered during the mine design stage, operators should perform moisture sensitivity tests on the material so the long-term stability of the mine is not jeopardized.

Acknowledgments

This work was conducted as part of the research program of the Office of Mine Safety and Health Research of the National Institute for Occupational Safety and Health (NIOSH). The findings and conclusions in this paper are those of the authors and do not necessarily represent the views of the National Institute for Occupational Safety and Health. Mention of company names, products, or software does not constitute endorsement by NIOSH.

References

[1] Esterhuizen GS, Dolinar DR, Ellenberger JL, Prosser LJ. Pillar and roof span design guidelines for underground stone mines. Pittsburgh, PA: NIOSH Publication; 2011. p. 1–64.
[2] Esterhuizen GS, MM Murphy. S-pillar-software for stone mine pillar design. Pittsburgh, PA: NIOSH; 2011.
[3] Murphy MM, Ellenberger JL, Esterhuizen GS, Miller T. Roof and pillar failure associated with weak floor at a limestone mine. SME Pre-print; 2015.
[4] Stacey TR, Page CH. Practical handbook for underground rock mechanics. Clausthal-Zellerfeld. Trans Tech Publications; 1986. p. 144.
[5] Hoek E, Carranza-Torres C, Corkum B. Hoek-brown failure criterion. In: Proceedings of the 5th NARMS-TAC conference. University of Toronto; 2002. p. 267–73.
[6] Esterhuizen GS, Ellenberger JL. Effects of weak bands on pillar stability in stone mines: field observations and numerical model assessment. In: Proceedings of the 26th international conference on ground control in mining. Morgantown, West Virginia: West Virginia University; 2007. p. 320–6.
[7] Zipf RK. Numerical modeling procedures for practical coal mine design. In: Proceedings of the 41st U.S. rock mechanics symposium. Alexandria, Virginia: American Rock Mechanics Association; 2006. p. 1–11.
[8] Esterhuizen GS. A Stability factor for supported mine entries based on numerical model analysis. In: Proceedings of the 31st international conference on ground control in mining. Morgantown, WV; 2012.